THE UNIVERSITY OF MANITOBA

IMAGE RECORDING AND RECONSTRUCTION BY CURVILINEAR HOLOGRAMS

Dennis K. Morland

A THESIS

SUBMITTED TO THE FACULTY OF GRADUATE STUDIES

IN PARTIAL FULFILMENT OF THE REQUIREMENTS FOR THE DEGREE

OF MASTER OF SCIENCE

IN

ELECTRICAL ENGINEERING

WINNIPEG, MANITOBA

R3T 2N2

May, 1973

ABSTRACT

This thesis deals with the problem of real image formation by curvilinear holograms. A review of the pertinent literature in the field of holographic imaging is presented. An exact integral equation formulation is derived to describe real image formation by an ideal curvilinear hologram of arbitrary shape. The integral is solved exactly for the two-dimensional case. EXPERIMENT 1 examines the real image field for a point source when measures are taken to reduce the effect of physical degradation factors. Results show that the large hologram aperture and short hologram-to-object distance yields the expected limited depth-of-focus. The lack of abberrations in the image verify the advantage of using plane wave reference and reconstruction beams. EXPERIMENT 2 uses a diffusely scattering object in an arrangement similar to that of EXPERIMENT 1 in order to determine the obtainable resolution as a function of the ratio of aperture size to hologram-to-object distance. Results indicate that the obtainable resolution is about 6.8% of that of the ideal diffraction limited system. EXPERIMENT 3 shows that special precautions must be taken with curvilinear holograms in order to duplicate the resolution obtainable with planar holograms. Finally, a summary of results is presented and some comments on the practicality and applications of imaging by curvilinear holograms is made.

ACKNOWLEDGEMENTS

I wish to extend my sincere appreciation to Dr. W.M. Boerner for the guidance and encouragement he has given me in preparing this thesis.

I also wish to thank Mr. Y.M. Antar for his helpful comments.

The financial support received from the National Research Council of Canada (Grant No. A7240) and a University of Manitoba Grant in aid of research for equipment expenses is gratefully acknowledged.

In conclusion, I wish to thank Mrs. S. Clubine for her cheerful and expert typing of the manuscript.

Dennis Morland

TABLE OF CONTENTS

LIST OF FIGURES

LIST OF PHOTOGRAPHS

LIST OF SYMBOLS

Greek Alphabet:

α	Wedge angle
$\alpha, \alpha_1, \alpha_2, \alpha_3$	Generalized Fourier frequency variables
β, γ, τ	Complex variables of integration
γ	Film gamma
δ	Delta function
∇^2	Laplacian operator
θ, θ''	Polar angles
λ	Wavelength
π	Pi (3.14159...)
ρ	Radial distance of observation point
ρ'	Radial distance of source point
ρ''	Radial distance of hologram point
σ	Pole in complex γ plane
ϕ	Polar angle of observation point
ϕ'	Polar angle of source point
ϕ''	Polar angle of hologram point
ω	Angular frequency

Latin Alphabet:

a	Diameter of aperture
Å	Ångstrom unit
BS	Beam splitter

C_1, C_2	Contours of integration
d	Distance between source and observation points
D	Diffusely scattering object
E	Emulsion
F	Fringes
G	Green's function
G	Granite optical bench
h	Complex variable of integration
$H_o^{(2)}$	Zero order Hankel function of second kind
i	$[-1]^{1/2}$
J_o	Zero order Bessel function
k	Wave number $2\pi/\lambda$
K	Kernel of image response
L	Lens
LG	Liquid Gate
M	First surface mirror
$\hat{n}$	Unit normal to hologram surface
O	Object
O	60X microscope objective
P, P_i, P_s	Source function
P	XYZ Positioner
PW	Plane wave
$\bar{r}$	Observation vector
$\bar{r}'$	Source vector

$\bar{r}''$	Hologram vector
R	Hologram to object distance
r	Denotes space in which real image is found
R_o	Absorber placed at point of convergence of reconstruction source
R	Rail type optical bench
S	Source
S_h	Hologram surface
SF	40X spatial filter with 25 micron pinhole
S'	Deformed hologram surface
t	Time variable
v	Denotes space in which virtual image term propagates
V	Volume of integration
(x,y,z)	Coordinate system

chapter one

INTRODUCTION

Holography is a process wherein the phase and amplitude information of a wave diffracted from a three-dimensional object can be recorded in such a way that a duplicate or a conjugate of the original object wave can be produced at a later time. Information storage is accomplished by recording an interference pattern produced by the superposition of coherent reference and object waves. Reconstruction is done by illuminating this wave recording, the hologram, with a reconstruction beam which closely matches the original reference beam.

The basic concept of holography was originated in 1948 by Dennis Gabor as a result of his research into high resolution electron microscopy [17,18]. The inspiration for this two-step, lensless wave-reconstructing microscopy came from the invention, many years previous, of the "X-ray microscope" by Sir Lawrence Bragg [4,5]. Gabor envisioned that by recording the unfocused wavefronts themselves, the resolution limit of the electron microscope might be reduced to perhaps 1 Å, thereby making atomic structures visible. The lack of sufficiently coherent sources of X-ray and electron beams has prevented such resolution from being achieved to date. However, it should be noted that in principle holography offers a method of realizing extreme resolution, diffraction limited imaging.

The ability of holograms to store and reproduce the total information

of an object wavefront allows it to function in a virtually limitless variety of information processing and wavefront manipulation systems, many of which do not directly involve imaging [7,8,13,14,20,54,61,63]. Such applications will not be considered here; rather, the hologram will be examined solely in its role as a generator of real and virtual images of arbitrary irregular objects. Special consideration will be given to the resolution obtainable in holographically produced real images of three-dimensional objects.

Imaging properties of holograms have been conventionally treated from the viewpoint of planar hologram shapes. This configuration greatly facilitates mathematical analysis, expecially if the "paraxial approximation" is used [14,61]. In particular, Fourier transform analysis can be readily applied, thus allowing the use of the powerful techniques and theorems of Communication Systems Theory [38,54].

Investigations of such planar holograms [33,46,47,48] have yielded the fact that the resolution spot size (depth of focus) of a reconstructed real image point is inversely proportional to the effective hologram size and directly proportional to the object to hologram distance. For example, Rayleigh's criterion [71] states that diffraction limited resolution of a small circular aperture is $0.61\lambda R/a$ for a disk of diameter a at a distance R from the object, radiating at wavelength λ, where the subtended cone angle is $a/2R<<1$. Thus, a high resolution real imaging system must record a large segment of the waves diffracted from the object. A theory of curved holograms

can show that, provided "perfect" holographic recording is assumed, the resolution obtainable in the real image depends on the segment of the object wavefront that is recorded, but not on the exact hologram shape. This feature makes the topic of curvilinear holograms extremely important in the field of high resolution imaging systems.

It is the purpose of this analysis to investigate further the properties of curvilinear holograms, particularily in regard to the generation of real images.

In the literature review, a summary will be made of the pertinent contributions, both theoretical and practical, in the field of holographic imaging, with particular emphasis on curvilinear hologram shapes.

The theoretical analysis will present an integral equation description of imaging by an arbitrary curvilinear hologram modeled by a thin variable transmittance film. This analysis will be modified by consideration of the properties of real recording media as they apply to curvilinear hologram shapes.

The experimental section will describe a number of experiments to investigate properties of real image formation. Experiments 1 and 2 will serve to determine how well the resolution obtainable in a holographically produced real image compares to the resolution of an ideal diffraction limited imaging system. Results will show that the obtainable resolution, while less than the ideal, is sufficient to enable

the real image of a diffusely scattering object to be constructed with great accuracy. Experiment 3 will investigate the difficulties encountered in obtaining the real image of objects from curvilinear holograms. Results will show that in general curvilinear holograms are much more susceptible to image degrading phenomena than are planar holograms.

Finally, a summary of results will be presented and some comments on the practicality and applications of imaging by curvilinear holograms will be made.

chapter two

LITERATURE REVIEW

The principle of wave recording by the interference pattern formed by the superposition of coherent reference and object waves was first conceived by Dennis Gabor in 1948 during his research into high resolution electron beam microscopy [17,18]. He described the recording made in this way as a hologram, from the Greek word "holos", which means "whole". The science involving such wave recordings then became known as holography. Several researchers attempted to improve the obtainable resolution [13] but achieved little success. This was due to the unavailability of sufficiently coherent sources which necessitated the use of an "in line" configuration and made it impossible to effectively separate the real image, virtual image and zero order transmittance terms in the reconstruction process.

With the advent of the optical laser and the "off-axis" techniques of Leith and Upatnieks in the early 1960's [38,39,40], the various image terms could be spatially separated. Leith and Upatnieks were also the first to consider holography from the viewpoint of Communication Systems Theory [38]. These innovations made holography an important, practical engineering tool.

Holograms may be considered under three main classifications according to the manner in which they are recorded. These are: Fresnel holograms, Fraunhofer holograms and Lensless Fourier Transform Holograms [20,61,63]. In general, the Fresnel hologram is formed relatively

close to the sources where the paraxial approximation [61] cannot be used. Fraunhofer holograms are formed in the far field, and lensless Fourier Transform holograms are formed using object and reference beams with equal divergent radii so that the recording assumes many of the characteristics of Fraunhofer holograms [63] (see Fig. 1).

Although holographic recordings are often considered as a two-dimensional transmittance function (i.e. a perfectly "thin" variable transmittance film), such an assumption is good for a first approximation only and in many cases leads to completely erroneous results [8,14]. It has been shown [41,44,61] that, since photographic emulsions in particular are many wavelengths thick, holograms recorded in them must be considered as a volume diffraction grating. Analysis of such thick emulsions [13, 61,30] have shown that the conjugate image is very strongly attenuated in reconstruction. Reflection type holograms [12,13,63] can be made, due to the volume effect, by having the reference and object beams intercept in a large (nearly 180°) angle so that the fringe period approaches half a wavelength. Such volume gratings will exhibit pronounced Bragg diffraction so that, with a white light reconstruction beam, the reconstructed images will be essentially monochromatic. The bandwidth of the reflected light has been found to be approximately 50Å [13]. The spatial frequencies normally encountered in cylindrical or conical hologram shapes necessitates consideration of the volume effect.

A serious problem in holography is the inadequacy of the recording materials which results in a loss of image resolution. Silver halide

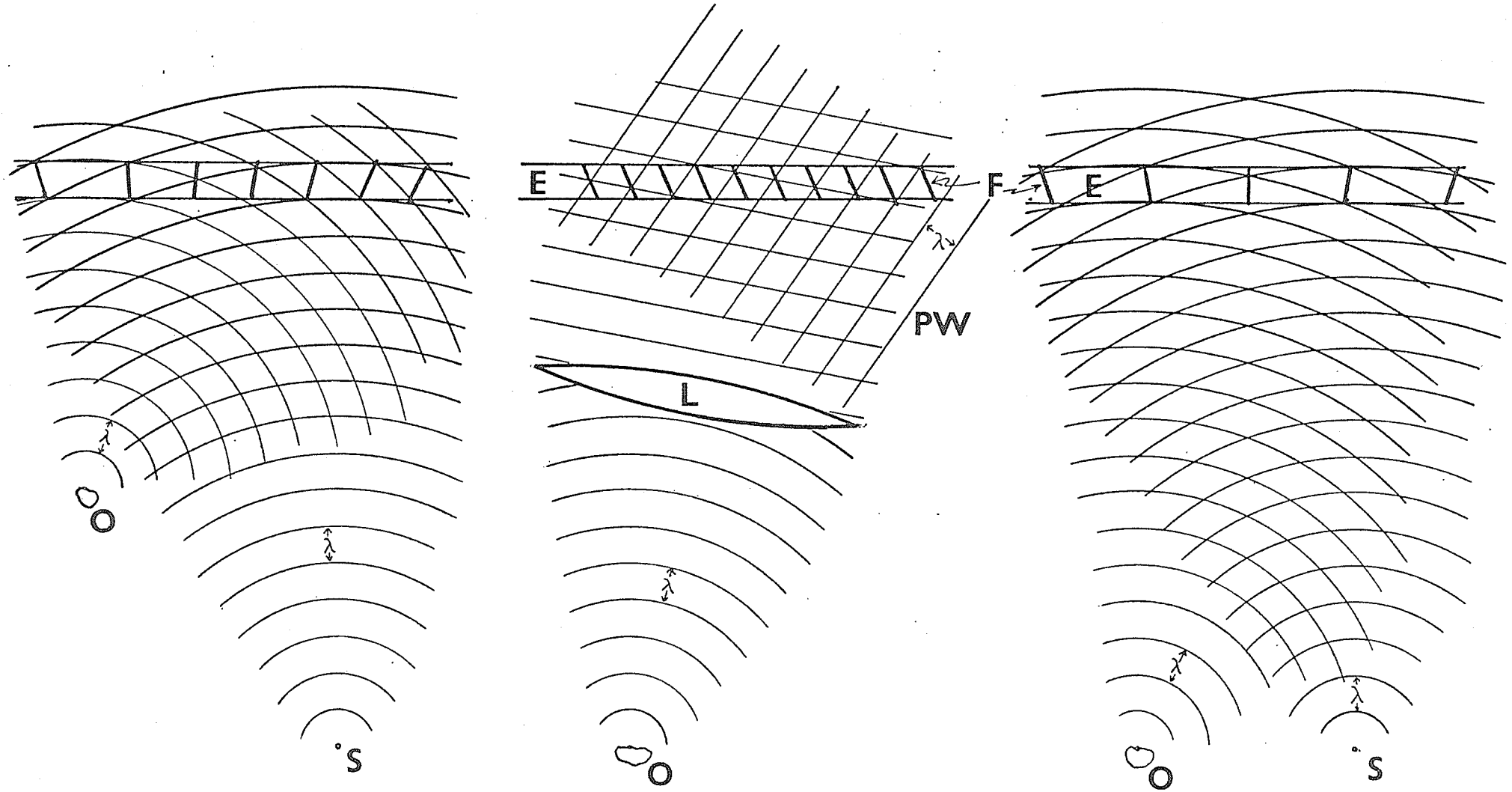

a) FRESNEL HOLOGRAM

FRINGE FREQUENCY VARIES

b) FRAUNHOFER HOLOGRAM

FRINGE FREQUENCY CONSTANT

c) LENSLESS FOURIER TRANSFORM HOLOGRAM

FRINGE FREQUENCY APPROXIMATELY CONSTANT

FIG.2.1 HOLOGRAM TYPES; (O) OBJECT, (S) POINT SOURCE, (E) EMULSION, (F) FRINGES, (L) LENS, (PW) PLANE WAVE.

recording materials are inherently noisy and resolution limited due to the finite film grain size. They are also prone to distortion due to the instability of the gelatin base. Several researchers [11,56, 34,21,43,25,13] have considered the effects of these phenomena. The nonlinearity of films [16,22,6,35,13] is another serious source of image degradation. A drawback of conventional absorption holograms is the fact that the high "bias" densities required for linear recording results in a strong attenuation of the reconstruction beam and a very low efficiency [21,61]. To overcome this problem another class of of holograms have been considered. These are "phase holograms" in which the intensity pattern is recorded as a variation in the index of refraction of a material rather than as a variation in absorptive density [61]. Latta [37] describes a method of obtaining phase holograms by chemically bleaching the processed,photographically recorded interference pattern. Others [31,13,57,9,66] experimented with a great variety of chemical bleaches. The effect of bleaching has been found to be a great increase in diffraction efficiency at the expense of image resolution and contrast [13,66]. Phase holograms have also been successfully recorded in other media including photochromic glasses [23,49], dichromated gelatins [42,58,13] and deformable thermoplastics [67,13]. These materials are very important for curvilinear holography since they offer higher resolution and less distortion than photographic films.

The possibility of object mensuration by holographic methods is an important one which has received a great deal of interest. In a series

of studies [48,47,46] Meier has shown that a holographic recording can contain sufficient information about an object scatterer to reproduce the scattering surface with a great deal of accuracy. Hildebrand and Haines [24] have proposed a method of measuring surface contours using multiple wavelengths or multiple sources. Bates [3] has experimented with constructing holograms with information gathered from X-ray analysis of objects and then regenerating the object profiles from the holograms. Mikhail [50,51] and McDonnell [45] have studied the feasibility of holographic mensuration and mapping from a photogrammetric point of view. Their technique involves manual scanning of the virtual image produced by a planar hologram to obtain the data samples. Although they have shown good accuracy with this method it has the disadvantages of being a very laborious procedure requiring highly complex instruments, subjective decision-making, and highly skilled personnel.

It is proposed that the mensuration system can be made much simpler, and perhaps automatic, if the real image is analysed instead of the virtual image. Stetson [62] used the limited-depth-of-focus effect [47,48] to generate the contour of a scattering object by intercepting the real image field from a planar hologram by another photographic film. Gara and Majkowski [19] are using a similar configuration to obtain the contours of clay models. Their system features a liquid gate to reduce film emulsion distortion and a digital sampling of the real image. Sherman [49], Wolf and Shewell [60,69] and Lalor [36] have also considered inversion of the field recorded on a planar surface.

The planar nature of most holograms permits only a limited perspective to be recorded. King [32] recorded a 360° view of an object on a planar hologram by making multiple exposures and rotating the object before each exposure. The reconstruction however still yields only a limited set of perspectives. True 360° recordings have been made by various authors [26,27,28,64,29] by surrounding the specimen by the recording film and illuminating it with a highly divergent wave. Only virtual images have been reported to date.

The images formed by such systems must be analysed by a theory of large-angle holograms to determine the increase in resolution. Mittra and Ransom [52], Wolf [68], Kozma and Zelenka [33] and Champagne [10] have considered nonparaxial imaging from large scale planar holograms. R.P. Porter [55] has shown that in curvilinear holograms, the resolution of the real image depends on subtended angle but not on aperture shape. His analysis, however, is restricted to two-dimensional holograms and further is based on the assumption of a perfect recording medium.

Clearly, a theory of three-dimensional curvilinear holograms is needed to determine the possible resolution of such a system and to predict the effect of practical limitations. It is suggested that the increased resolution and the limited depth of field obtained in a 360° hologram can be used to advantage for the purpose of object mensuration ("close-up" photogrammetry). Digitalization of the real image by a scanning photodetector may then enable the object shape to be retrieved automatically.

chapter three

ANALYSIS OF CURVILINEAR HOLOGRAMS

3.1 INTRODUCTION

The analysis is restricted to a two-step imaging process. In the first or recording step, a reference point and an object source with known radiated or scattered fields is assumed to be surrounded by a transparent recording medium of arbitrary shape. The superposition of the coherent reference and object waves produces a stable interference (intensity) pattern which is recorded by this medium. The recording is processed so that the interference pattern is represented by a variable transmittance. In the second or reconstruction step, the object and reference sources are removed and the hologram is illuminated by the conjugate of the reference wave to create a real image.

A theory of curved holograms can show that the resolution of the real image depends on the segment of the object radiation subtended by the hologram surface but not on the surface shape. An exact, integral formulation of diffraction theory is used to represent the image field produced by the hologram. The point reference hologram, whose recording arrangement is shown in Fig.3.1, is modelled by a collection of surface sources analogous to a charge and dipole layer. The surface sources can be derived from the film transmittance [55].

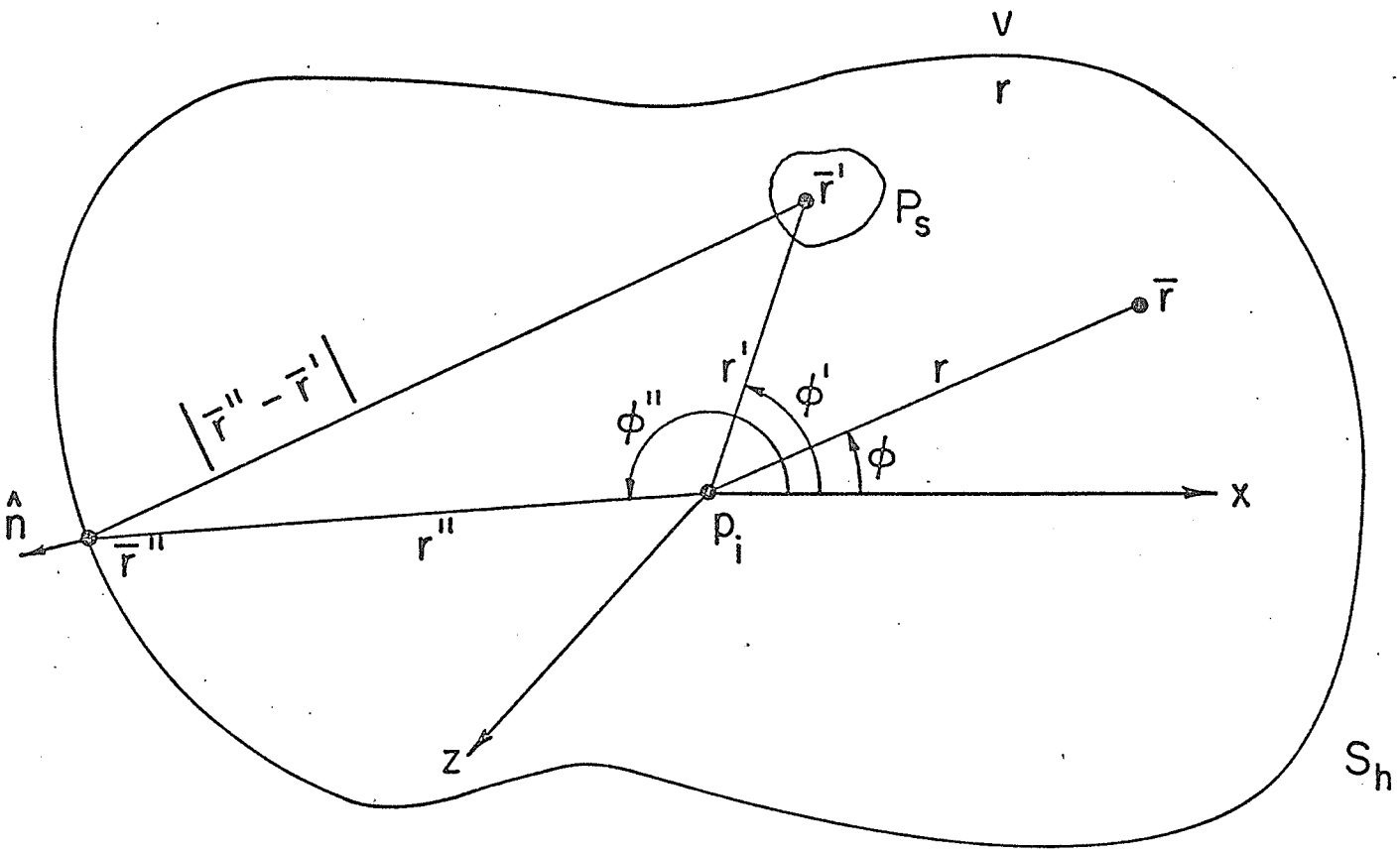

FIG. 3.1 GEOMETRY FOR A HOLOGRAPHIC SURFACE S_h OF ARBITRARY SHAPE.

Section 3.2 presents the three-dimensional Green's function formulation of diffraction theory. The basic image system is defined and analysed in Section 3.3. Section 3.4 presents the model of a point reference hologram. Section 3.5 is a brief discussion of the effects of physical characteristics of holograms on real image construction.

3.2 THREE-DIMENSIONAL GREEN'S FUNCTION FORMULATION

The theory presented here is restricted to the complex monostatic, time-independent, scalar wave equation

$$(\nabla^2 + k^2)\psi(\bar{r}) = -p(\bar{r}) \quad , \tag{1}$$

where k is the wavenumber $2\pi/\lambda$ and λ is the wavelength of the radiation.

For the time dependence $\exp(i\omega t)$ and a lossless, isotropic medium, the scalar Green's function [71] that satisfies

$$(\nabla^2 + k^2)G(\bar{r},\bar{r}') = -\delta(\bar{r} - \bar{r}') \quad , \tag{2}$$

is

$$G(\bar{r},\bar{r}') = \frac{\exp(-ik|\bar{r} - \bar{r}'|)}{4\pi|\bar{r} - \bar{r}'|} \quad , \tag{3}$$

where $\bar{r}'$ denotes the source coordinates and $\bar{r}$ denotes the observation coordinates. If the response to a finite source $p(\bar{r})$ satisfies the Sommerfeld radiation condition and is unique and linear[75], the field due to a collection of such sources is

$$\psi(\bar{r}) = \int_V p(\bar{r}')G(\bar{r},\bar{r}')dV' \quad , \tag{4}$$

where the integral is over the volume V that contains all the sources. The basic image system and the transmission hologram can be defined by

specifying the field difference across the hologram. With reference to Fig.3.1, the surface sources are related to the discontinuities in the field by the relations

$$\psi_r(\bar{r}'') - \psi_v(\bar{r}'') = \sigma_1 \quad , \tag{5}$$

$$\hat{n}\cdot[\nabla''\psi_r(\bar{r}'') - \nabla''\psi_r(\bar{r}'')] = \sigma_o \quad , \tag{6}$$

where ψ_r and ψ_v are evaluated in the r and v spaces of Fig.3.1 and where ∇'' is the gradient in $\bar{r}''$ coordinates. Equations (5) and (6) are the boundary conditions, given by Maue [74], for the scalar wave equation and σ_o and σ_1 are zero and first order surface singularity sources respectively. These surface sources can be used to find the field on either side of an arbitrary surface S_h by substituting the sources into Eqn.(4) and then performing the integration across the surface in the direction of its unit normal $\hat{n}$ [74].

The field is

$$\psi(\bar{r}) = \left\{ \begin{array}{ll} \psi_r(\bar{r}) & \bar{r} \text{ in r space} \\ \psi_v(\bar{r}) & \bar{r} \text{ in v space} \end{array} \right\}$$

$$= \int_{S_h} \{\sigma_o G(\bar{r},\bar{r}'') - \sigma_1 \hat{n}\cdot\nabla'' G(\bar{r},\bar{r}'')\} dS''. \tag{7}$$

3.3 BASIC IMAGE SYSTEM

The basic image system, as defined by Porter [55], is the collection of zero and first order sources on a surface, surrounding the location of the object during the first step, that form an image of a point object by launching a converging spherical wave during the second step. With reference to Fig.3.1, the converging wave is launched

from the hologram surface S_h and forms a real image in the r space, inside S_h. This image forming wave then diverges and passes out of the hologram surface into the v space, outside S_h (Fig.3.1). The image forming field of a point source, the point response of the system, is called the kernel and is denoted by K.

The image kernel for an arbitrary hologram surface S_h can be determined from Eqn.(7). The appropriate zero and first order sources, $\hat{n}\cdot\nabla''G^*(\bar{r}'',\bar{r}')$ and $G^*(\bar{r}'',\bar{r}')$, are found by substituting the appropriate Green's function into Eqn.(5) and Eqn.(6). The real image kernel has been found by Porter [55] to be

$$K_r(\bar{r},\bar{r}') = \int_{S_h} \{G(\bar{r},\bar{r}'')\nabla''G^*(\bar{r}'',\bar{r}') - G^*(\bar{r}'',\bar{r}')\nabla''G(\bar{r},\bar{r}'')\}\cdot\hat{n}dS'' \quad (8)$$

Following Eqn.(4), the real image field can be written in terms of this kernel as

$$\psi_r(\bar{r}) = \int_V p^*(\bar{r}')K_r(\bar{r},\bar{r}')dV' \quad (9)$$

by the principle of superposition.

Since S_h will be considered here to be in general a cylindrical shape, the three-dimensional Green's function will be represented in a more appropriate form. As shown in *appendix* A.1, the Green's function can be written as

$$\frac{\exp(-ik|\bar{r} - \bar{r}'|)}{4\pi\ \bar{r} - \bar{r}')} =$$

$$= \frac{-i}{8\pi}\int_{-\infty}^{\infty} H_o^{(2)}([\rho^2+\rho'^2-2\rho\rho'\cos(\phi-\phi')]^{1/2}[k^2-h^2]^{1/2})\exp(ih|Z-Z'|)dh \quad , \quad (10)$$

where we have used

$$|\bar{r} - \bar{r}'| = [\rho^2+\rho'^2-2\rho\rho'\cos(\phi-\phi') + (Z-Z')^2]^{1/2} \quad . \quad (11)$$

We may now consider the case where the hologram surface S_h only partly surrounds the object. With reference to Fig.3.2, consider a hologram surface that is asymptotic to a wedge of angle α at infinity. For $\bar{r}$ and $\bar{r}'$ to the right of S_h in Fig.3.2, the divergence theorem can be used to show

$$\int_{S_h} \{\quad\} \cdot \hat{n}dS'' = \int_{S'} \{\quad\} \cdot \hat{n}dS'' \quad , \quad (12)$$

where the integrand is that of Eqn. (8).

The integration can be simplified if S' is deformed to an arc of a circle of radius ρ'' centered at the object point, since in this case the unit normal to the surface S' has a radial component only. For large ρ'' , we can use the approximation to the zero order Hankel function of the second kind

$$H_o^{(2)}(\beta\rho'') = [\frac{2}{\pi\beta\rho''}]^{1/2}\exp(-i(\beta\rho'' - \pi/4)) \quad , \quad (13)$$

$$\rho'' \to \infty$$

where $\beta^2 = k^2 - h^2$.

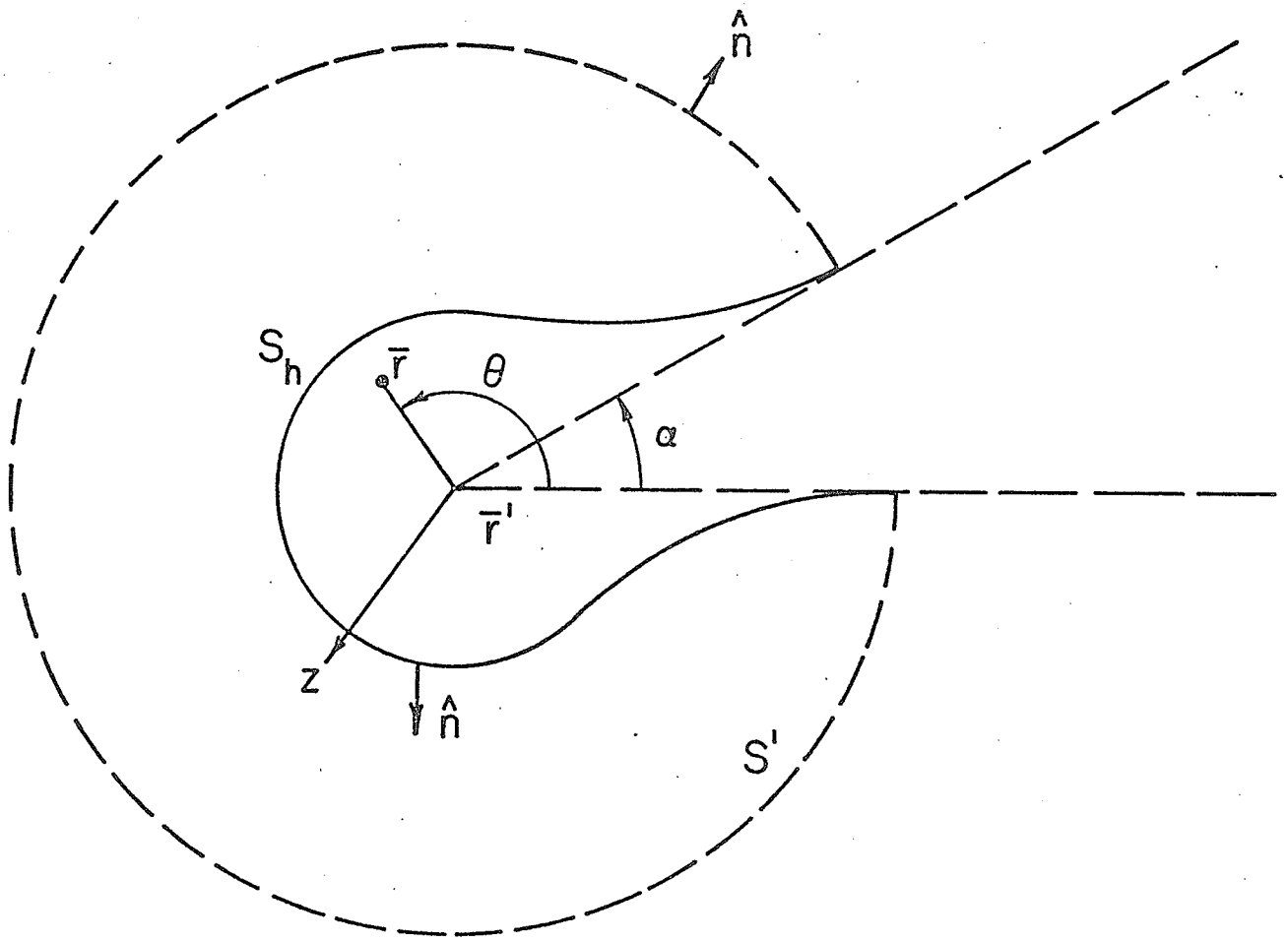

FIG. 3.2 GEOMETRY FOR OPEN HOLOGRAM ASYMPTOTIC TO WEDGE OF ANGLE α.

Defining $d = |\rho - \rho'|$ and using the approximation to the cosine law $|\rho - \rho''| = [\rho'' - d\cos(\theta'' - \theta)]$, see Fig.3.2, we can write the kernel in the r space as

$$K_r(\bar{r},\bar{r}') \cong \frac{i}{16\pi} \int_{S'} \Big[\{\beta^{-1/2}\exp(-i\beta[\rho''-d\cos(\theta''-\theta)])\exp(ih|Z-Z''|)dh\}$$

$$\times \{\int_{-\infty}^{\infty} \beta^{+1/2}\exp(i\beta\rho'')\exp(-ih|Z''-Z'|dh\}$$

$$-\{\int_{-\infty}^{\infty} \beta^{-1/2}\exp(i\beta\rho'')\exp(-ih|Z''-Z'|dh\} \quad \times$$

$$\{\int_{-\infty}^{\infty} \beta^{1/2}\exp(-i\beta(\rho''-d\cos(\theta''-\theta)))\exp(ih|Z-Z''|)dh\}\Big]d\rho''d\theta''dZ'' \qquad (14)$$

As Sherman [59] has noted in similar problems, it is very difficult to evaluate such integrals to find the image kernel. However, since we are primarily interested here in finding the resolution as a function of the angle α, we can easily solve the equation for the two-dimensional (ρ,ϕ) case to find the kernel in the r space as

$$K_r(\bar{r},\bar{r}') = \frac{i}{4\pi} \int_{\alpha}^{2\pi} \exp[jkd\cos(\theta'' - \theta)]d\theta'' \,. \qquad (15)$$

The kernel depends only upon the wedge angle α and not on the exact shape of S_h. When $\alpha = o$, the kernel becomes

$$K_r(\bar{r},\bar{r}') = \frac{i}{2} J_o(kd) \,. \qquad (16)$$

3.4 MODEL OF POINT REFERENCE CYLINDRICAL HOLOGRAM OF INFINITE EXTENT

Consider Fig.3.1 with the coordinate system centered on the reference source located at R_o, with $\bar{r}''$ the variable distance from the film to the point source. The total radiated field on the film is

$$\psi_o(\bar{r}'') = \psi_S + \exp(-ik\bar{r}'') \; / \; 4\pi\bar{r}'' \tag{17}$$

where ψ_S is the field radiated from the object source P_S. The recording medium is sensitive to the irradiance

$$I = \frac{1}{2}\,\psi_o\psi_o^* \quad , \tag{18}$$

which is the time average of the square of the field [71]. If we assume that the object field is very much less than the reference field, we can write

$$I \cong \frac{1}{2}\left[\frac{1}{(4\pi\bar{r}'')^2} + \frac{\psi_S^*\exp(-ik\bar{r}'')}{4\pi\bar{r}''} + \frac{\psi_S\exp(ik\bar{r}'')}{4\pi\bar{r}''}\right]. \tag{19}$$

If this intensity pattern is recorded by a photographic emulsion, the processed film can be described, to a first approximation, by a transmittance $T \cong AI^{\gamma}$ [14,61]. Here, γ is the developing exponent, assumed to be one, and A is a film-exposure coefficient that can vary from point to point along the film.

The reference field is reconstructed when the film-exposure coefficient is

$$A \propto 2(4\pi\bar{r}'')^2 \tag{20}$$

Without loss of generality, the proportionality constant will be taken as one.

Therefore the transmittance is

$$T = 1 + 4\pi\bar{r}'' \left[\psi_S \exp(ik\bar{r}'') + \psi_S^* \exp(-ik\bar{r}'')\right]. \tag{21}$$

To form the real image, the film must be illuminated from the outside by a converging wave $\exp(ik\bar{r}'')/4\pi\bar{r}''$. The field in the r space of Fig.3.1 during reconstruction then becomes as shown in Fig.3.3

$$\psi = T \frac{\exp(ik\bar{r}'')}{4\pi\bar{r}''} \tag{22}$$

$$= \frac{\exp(ik\bar{r}'')}{4\pi\bar{r}''} + \psi_S^* + \psi_S \exp(2ik\bar{r}'') + \psi' \,, \tag{23}$$

where ψ_S^* is the converging real image field and ψ' is the field diverging from the real image. The first and third terms in Eqn.(23) will be spatially separated from the image term if $\bar{r}'$ has a sufficiently large Z' component [61]. That is, they will be separated if the object and source points are widely separated on the Z-axis.

The resolution obtainable in the ideal case of a cylindrical hologram of infinite extent can be determined if we let the field ψ_S be the radiation from a point object at $\bar{r}'$, the free space Green's function [71], given in Eqn.(3). The converging wave must then be the complex conjugate of this function, $G^*(\bar{r},\bar{r}')$. For a point object at $\bar{r}'$, the real image field will be

$$\psi_r = G^*(\bar{r},\bar{r}') + \psi' \,, \tag{24}$$

where ψ' is the field diverging from the image. Since ψ_r must

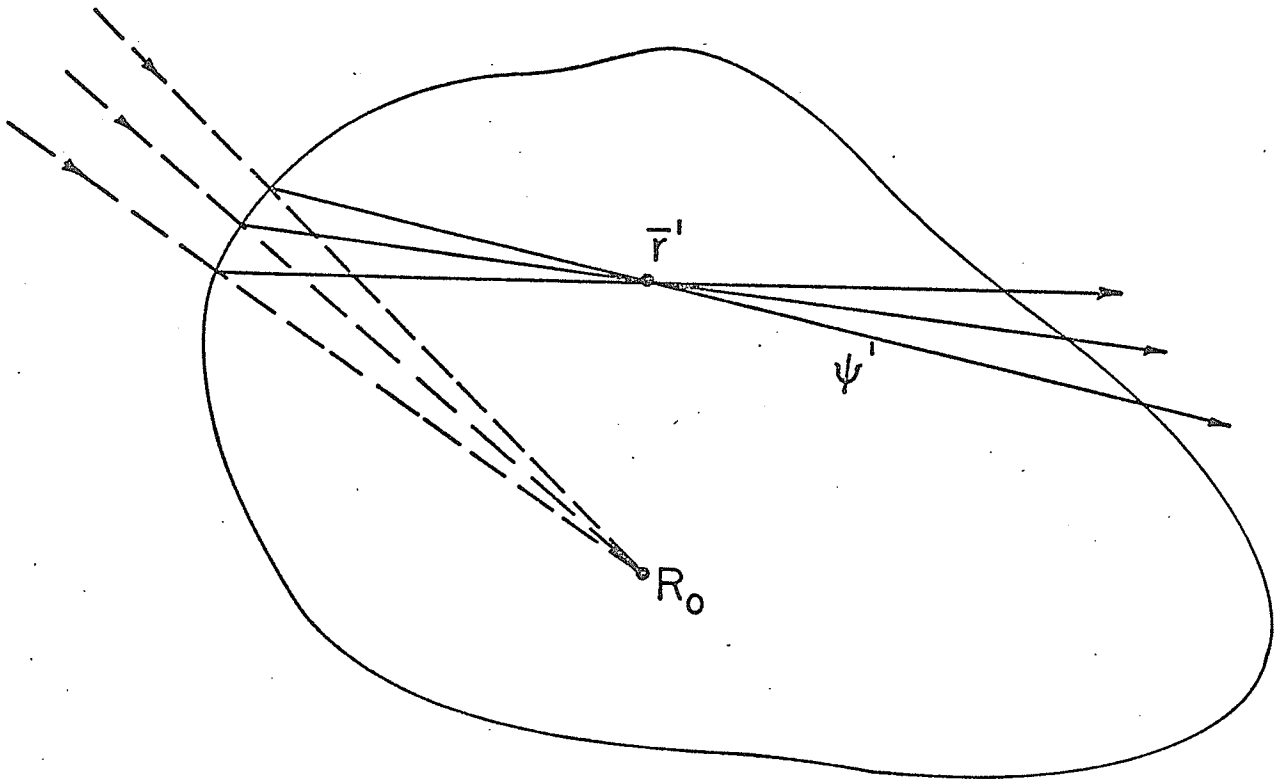

FIG. 3.3 HOLOGRAM ILLUMINATED BY RECONSTRUCTION SOURCE AND BY THE FIELD ψ' DIVERGING FROM THE IMAGE AT $\bar{r}'$

satisfy the homogeneous scalar wave equation (i.e.Eqn.(1) with the source equal to zero), then we find that

$$(\nabla^2 + k^2)\psi'(\bar{r},\bar{r}') = \delta(\bar{r} - \bar{r}'). \tag{25}$$

From Eqn.(2) it is obvious that $\psi' = -G(\bar{r},\bar{r}')$. Therefore the image field in the r space is

$$\psi_r = G^*(\bar{r},\bar{r}') - G(\bar{r},\bar{r}') \quad . \tag{26}$$

Substituting Eqn.(3) into Eqn.(26) yields the result

$$\psi_r = \frac{i}{2\pi} \frac{\sin(k|\bar{r}-\bar{r}'|)}{|\bar{r}-\bar{r}'|} \quad . \tag{27}$$

This function represents an impulse at the point $\bar{r}'$. According to the Rayleigh criterion [71], the resolution, and hence the depth of focus, is equal to twice the distance between the maximum and the first minimum of Eqn.(27), which is $\lambda/2$. Since the volume of the image point in Eqn.(27) does not change as a function of $\bar{r}'$, then the system is an ideal isoplanatic one.

3.5 DISCUSSION

As demonstrated in the above analysis, the theoretical maximum resolution of a large-extent cylindrical holography system is on the order of the wavelength of the light involved. In any real system many sources of distortion of the wavefronts (to be listed in *chapter four*) will combine to reduce the available resolution by a large amount. However, the resolution of the system could be decreased by a hundred-